# We are IntechOpen, the world's leading publisher of Open Access books Built by scientists, for scientists

6,900
Open access books available

185,000
International authors and editors

200M
Downloads

Our authors are among the

154
Countries delivered to

TOP 1%
most cited scientists

12.2%
Contributors from top 500 universities


WEB OF SCIENCE™

Selection of our books indexed in the Book Citation Index in Web of Science™ Core Collection (BKCI)

## Interested in publishing with us?
## Contact book.department@intechopen.com

Numbers displayed above are based on latest data collected.
For more information visit www.intechopen.com

Chapter 2

# Ultra-Wideband FSS-Based Antennas

Rabia Yahya, Akira Nakamura and Makoto Itami

Additional information is available at the end of the chapter

http://dx.doi.org/10.5772/intechopen.79888

**Abstract**

As antennas are indispensable elements in wireless systems, it is necessary to provide UWB antennas suitable for UWB systems. The most proposed UWB antennas have omnidirectional radiation, which provides the wide coverage area that is highly demanded by many conventional UWB applications. However, directional radiation is more beneficial for other UWB applications and it may even be beneficial for the conventional UWB omnidirectional applications in some environments that contain many sources of interference and distorting objects, where the omnidirectional radiation leads to high interference and loss of power in undesirable directions. Consequently, an immense research has addressed the issue of realizing UWB planar antennas with unidirectional radiation characteristics. Basically, the main technique used to create unidirectional radiation patterns is employing cavity-baking reflectors to redirect the back radiation, hence increasing the gain of the radiators. In addition, these reflectors can decouple the mounted radiator from the surroundings that can damage its characteristics. Therefore, we suggest the employment of UWB reflectors to achieve UWB planar antennas with directional radiation. Our research for designing optimal UWB reflectors has led to the investigation in the field of frequency selective surfaces (FSSs), which are valuable structures and can be of great interest to a wide range of applications especially UWB applications. Subsequently, the main aim of this chapter is to give a review of the fundamental uses of FSSs in antenna engineering and the basic physical concepts that have been employed to serve the purpose of enhancing antennas' performances using FSSs with a variety of features and characteristics. Furthermore, it is geared toward the presentation of our proposed UWB FSS-based antennas. First, we use basic FSSs such as the capacitive and its complementary inductive FSSs to design UWB reflectors that can serve improving and stabilizing the gain of UWB antennas. Thereafter, a proposed UWB single-layer FSS is used to serve the same purpose. Then, the FSS is integrated and designed together with UWB radiator, which resulted in lower profile along with good performance.

**Keywords:** FSS, UWB reflectors, UWB FSS, directional UWB antennas, unidirectional radiation

IntechOpen

© 2018 The Author(s). Licensee IntechOpen. This chapter is distributed under the terms of the Creative Commons Attribution License (http://creativecommons.org/licenses/by/3.0), which permits unrestricted use, distribution, and reproduction in any medium, provided the original work is properly cited. CC BY

## 1. Introduction

The antenna is an important aspect of any wireless system. It ensures the transmission/reception of the signals and can be designed to comply with the systems' requirements, especially those with imposed regulations that must be respected such as UWB systems. Antennas are the components of the wireless communication system that are responsible for shaping and launching the emission as well as receiving the incoming radiation. As a result, the system's antennas control its coverage range and area. As the antenna directivity gets increased, its coverage area gets narrower, which may not be convenient for omnidirectional applications. Meanwhile, many real-world environments cause the distortion of the omnidirectional radiation and make it more exposed to interference with the surroundings. Hence, in these cases, the directional radiation becomes preferable, especially when it ensures a wiser use of the radiated power.

Appropriately designed UWB reflectors can bring directionality to existing UWB omnidirectional antennas, as well as shielding them from nearby metallic objects that would otherwise destroy their performance, providing them with the suitability for a variety of applications. It is obvious that planar metallic reflectors cannot provide these advantages over an ultra-wide bandwidth due to their out-of-phase reflection.

Developments in periodic structures have led to the development of planar surfaces that have, among other characteristics, the possibility to act as a perfect magnetic conductor (PMC) with in-phase reflection over a narrow bandwidth. The insertion of such surfaces enhances impedance matching, hence improving the efficiency of some antennas (e.g., printed planar antennas) when they have to be installed close to conducting surfaces, and creates a unidirectional radiation. These structures can be seen as a combination of frequency selective surfaces (FSSs) and conventional metallic reflectors. FSSs have helped to solve some crucial challenges in various fields and they have been proposed as UWB reflectors.

Furthermore, by proposing UWB FSSs, the applications of these structures can be extended to include UWB communication systems and radars or to enhance the performance of UWB components such as antennas, where UWB FSSs can be used as UWB reflectors to increase their gain and minimize their back radiation and create pattern diversity.

This chapter is a compendium of FSSs in antenna engineering that gives an introduction to how FSSs have been used in antenna fields and their potentials that can serve our purposes. Furthermore, it illustrates the principal physical concepts that can be used to explain the interaction between antennas and FSSs. Then, it itemizes the designs of the proposed FSS-based antennas using the concepts introduced in the first part.

## 2. Relations between FSSs and well-known structures

Some well-known structures, such as high impedance surfaces (HIS), can be considered as evolved versions of FSSs, whereas these structures combine FSSs with metallic ground planes and metallic pins (vias). Hence, they can provide two important characteristics, namely, artificial magnetic conductor (AMC) and electromagnetic band gap (EBG) simultaneously.

An FSS of metallic patches, like the one indicated in **Figure 1**(**a**), can effectively suppress surface waves because currents cannot travel across the gaps between the patches. Over the frequency range where it prohibits surface waves, it is partially reflective. It is only at very high frequencies, when the effective capacitors between neighboring plates behave as shorts, that surface waves can propagate. Hence, this FSS transmits low frequencies while reflecting high frequencies.

The complementary geometry of this capacitive FSS is the inductive one that consists of an array of square slots as shown in **Figure 1**(**b**). Since the inductive structure represents the complementary of the capacitive one, it has complementary transmission spectra. Thus, the latter transmits high frequencies while reflecting low frequencies.

For the inductive surface, the waves that are short compared to the diameter of the holes will easily fit through the mesh, while longer waves will see the sheet as continuous metal. Therefore, the sheet of metal islands transmits long wavelengths while reflecting short wavelengths. At low frequencies, where it can prevent the propagation of surface waves, the capacitive sheet is not completely reflective. Conversely, while the inductive sheet is reflective at low frequencies, surface waves can propagate easily along the continuous metal wires.

If a ground plane is added to a capacitive FSS, the structure will become completely reflective, and it will own the favorable reflection phase properties of high-impedance surfaces, but the propagation of surface waves will still be permitted. It is only when both the ground plane and the vias are included that the important properties of high-impedance surfaces, namely, in-phase, 100% reflection, and suppression of surface current propagation, are obtained [1].

### 2.1. FSS in proximity to a ground plane

Free-standing doubly periodic arrays of metallic elements were studied for many years in the context of FSS and their behavior is well understood. The incident polarization is assumed to be suitable to excite the metallic elements, meaning that in the case of linear dipole elements,

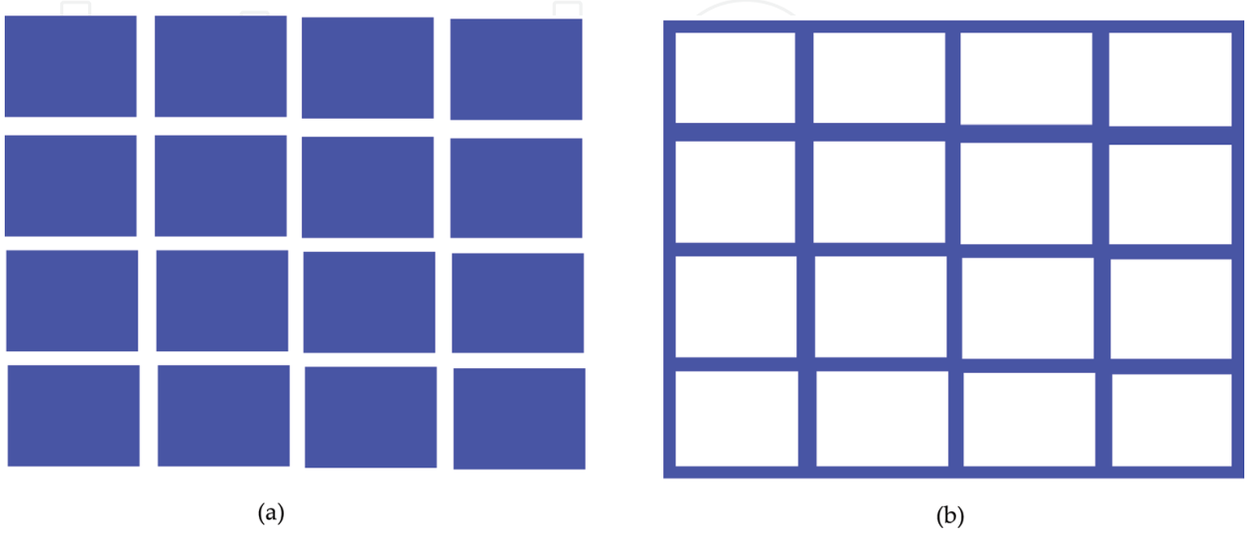


**Figure 1.** Complementary surfaces. (a) Capacitive surface, (b) inductive surface.

the electric field should have a component parallel to the direction of the dipoles. It is well known that at the resonant frequency of the array, the latter performs as a fully metalized screen and the incident waves are fully reflected with a phase reversal. Moreover, at resonance, the current is in phase with the incident field, i.e., the impedance seen by the incident wave is purely real, since the capacitive and inductive parts cancel each other. Also, a maximum current magnitude is excited on the elements.

For periodic arrays in proximity to a ground plane, some differences emerge. Due to the ground plane, incident waves are fully reflected at all frequencies. However, in this type of structures, careful investigation reveals that two distinct resonant phenomena occur for a normally incident wave. By assuming a free-standing array in proximity to an all-metal ground plane illuminated by a normally incident wave, the array resonance can be defined at the frequency where the currents excited on the array are in phase with the incident wave. At this frequency, the incident wave is reflected from the periodic array with a phase reverse, as in the case of the free-standing array resonance. However, it can be found that there also occurs a Fabry-Perot type of resonance at the cavity formed between the ground plane and the array. The Fabry-Perot resonance occurs at frequencies different from the array resonance. This strong cavity-type resonance excites maximum currents on the elements (which in general are out of phase with the incident wave), and the incident wave is reflected with a zero phase shift [2].

### 2.2. AMC resonance cavity

The presence of vias in a mushroom-type structure imposes an EBG at the same frequency range as the AMC property. In other words, the mushroom structure exhibits high surface impedance for both normally incident and surface waves at the same frequency band. Hence, at the same frequency, it reflects a normally incident plane wave with zero phase shift behaving, therefore, as an AMC and supports no surface waves behaving, therefore, as an EBG. It was demonstrated that the AMC operation is not directly related to the resonance of the FSS array. In fact, it is noticed that with varying array periodicity, the AMC band moves oppositely to the FSS resonance frequency. On the contrary, it is shown that the EBG frequency follows the trend of the FSS resonance [2].

### 2.3. Complementary arrays

It can be shown that the specular reflection coefficient for one array equals the transmission coefficient for its complementary array. This is a simple case of the general "Babinet's principle." Based on this observation, it is often expected that the investigation of one of the two cases is enough. However, this is in general not the case. First of all, the conducting screen must be a perfect conductor and "infinitely" thin, typically less than 1/1000 wavelength. If the screen is thick, the bandwidth of the dipole array will be larger while the bandwidth of the slot array will be smaller. Furthermore, if a thin layer of dielectric is added, the resonant frequency will be lowered somewhat for both the dipole and the slot arrays, but for a dielectric thickness of the order of $\lambda/4$ or more, the two cases behave vastly different [3].

## 3. FSSs in antenna engineering

FSSs' valuable features emphasized through the analysis above have encouraged their use in antenna engineering to improve antenna performance and create further properties that would not be achievable otherwise. They have been used, to widen the operating band of backing reflectors and to enhance the performance of broadband reconfigurable antennas, as superstrates and as reflectors.

### 3.1. FSSs as reflectors and ground planes

Extending the bandwidth of backing reflectors is among the rich utilizations of FSSs. In [4], an FSS is sandwiched between a tightly coupled array and a metallic plane, providing an additional reflecting plane for a higher frequency band. In this way, the metallic ground plane will operate at lower frequencies and the FSS will cover higher frequencies, which leads to an extended bandwidth, while the location of the metallic plane without an FSS would be suitable only for a relatively limited frequency range.

Placement of the metallic plane at a quarter wavelength distance from the antenna allows obtaining a good matching with only modest degradation of the achievable gain, but the improvement of the front-to-back ratio will come at the expense of the antenna bandwidth. The targeted application in [4] forces the integration of two frequency bands: one corresponding to the typical radar X-band, 8.50–10.50 GHz, and the other corresponding to a Tactical Common Data Link (TCDL) system, 14.40–15.35 GHz. Therefore, the used FSS was designed to be reflective at the higher frequency range and to be practically transparent for the lower band where the metallic ground plane is in charge of the reflection. More importantly, the FSS should separate the two frequency bands. Therefore, a special FSS has been chosen to serve the design purposes. The chosen element exhibits a good performance against angular variation and allows a packed lattice, with a further gain in angular independence.

In [5], a novel FSS design aimed at enhancing the performance of a broadband reconfigurable antenna has been presented. Designing FSSs' subject to phase requirements was also elaborated, revealing that some compromise, in the response magnitude, should be made to achieve the desired phase requirements. The broadband requirements also presented the need for noncommensurate FSS designs, contrary to previous FSSs that were primarily designed on the basis of the reflection coefficient amplitude and were intended for radome applications rather than substrates. When traditional broadband antennas such as log-periodic are printed on substrates, their bandwidth characteristics are altered, and one approach to regain the broadband behavior of the antenna element is to employ frequency-dependent substrates or ground planes (GPs). From here comes the suggestion of using FSSs to create substrates on which broadband antennas can be printed without affecting their broadband behavior. This can be achieved by using multiple layer FSSs as part of the substrate in a similar manner to that used for designing broadband microwave filters. Each screen is resonant at a given frequency and is placed at a distance, of a quarter of the wavelength at the screen's resonance frequency, away from the antenna's surface.

### 3.2. FSSs as UWB reflectors

In [6], a reflector consisting of two layers separated by an air gap of a width of 9.5 mm has been proposed. The upper layer was designed to be reflective over high frequencies of the UWB band and the second layer (lower layer) was used to reflect the transmitted waves through the upper layer. In other words, the upper layer operates as a band-stop filter for higher frequencies and a band-pass filter for lower frequencies, and the lower layer has an opposite operation.

In order to gain insights into the operation mechanism of multilayer FSS/antenna combination, a schematic describing the operating principle is presented in **Figure 2**. Two reference planes have been defined, namely, plane R and plane T. To obtain a prescribed phase variation, the dual-layer FSS has been optimized over the ultra-wide band. The upper layer, which is responsible for providing reflection at higher frequencies, is formed by a set of cross dipoles and square loops. The reflection phase from upper layer is noted by $\phi_1$, $\phi_2$ is the reflection phase provided by the lower layer, and $\phi_R$ is the overall phase reflected from the multilayer FSS at the reference plane R.

When an antenna is placed at a distance L (mm) above the FSS, the wave radiated toward the FSS is reflected. This reflected radiation would be added to the direct outgoing wave radiated

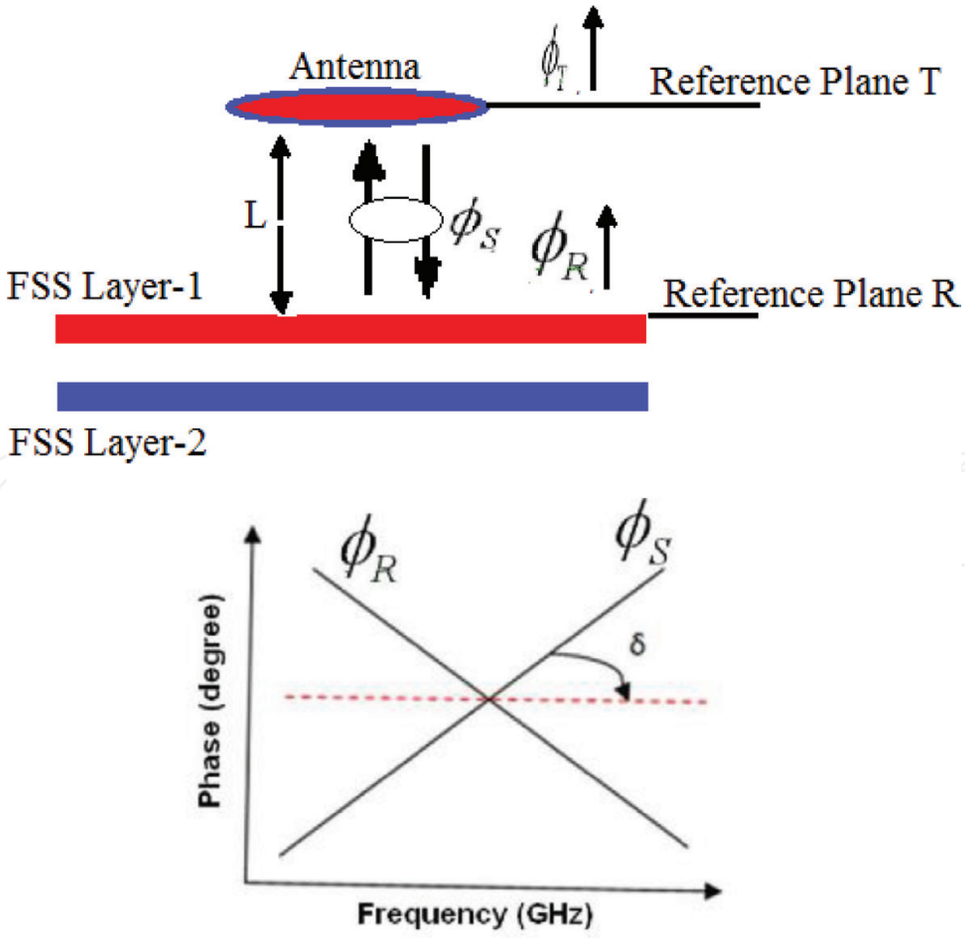


**Figure 2.** Operation mechanism of the dual-layer UWB reflector in [6].

from the antenna in the opposite direction to the FSS reflector. It is expected that the gain of the antenna in the presence of the FSS reflector will be maximum when the two wave components are added in phase, giving rise to constructive interference.

The evaluation of the phase at the reference plane T is described by the following equations:

$$\phi_T = \phi_R + \phi_S \tag{1}$$

where $\phi_R = f(\phi_1; \phi_2)$ at reference plane R and $\phi_S = 2 \times \frac{2\pi f}{C} L$ is the round-trip free-space propagation phase delay between the antenna and the top of the FSS reflector.

Note that, for phase coherence, $\phi_T$ should be zero (or an integral multiple of $\pi$) at all frequencies.

Since the phase delay is frequency dependent and increases with frequency, the ideal FSS reflection phase should decrease with frequency at the same rate, which is associated with the slope of the curve (lower plot in **Figure 2**) that is controlled by the spacing between the antenna and reflector.

Several UWB antennas have been located above this reflector to verify its functionality. In [7], the antenna was located at 10 mm, which is approximately λ/4 at the center frequency of 6 GHz, above the reflector and a maximum gain of 9.5 dBi was achieved at 4.2 GHz. The gain variation, over the frequency band from 3 to 10 GHz, was ±1.5 dB. In [8], a rectangular slot antenna, fed through microstrip rectangular patch, was employed as a radiator. An optimized height of 10 mm was chosen to separate the antenna structure from the FSS. It was revealed that the optimized UWB FSS reflector has a very small effect on the impedance bandwidth of the radiator, which is 145% with reflector and 149% without it, while the gain was significantly improved due to the reflector. The average peak gain achieved by the slot antenna alone is 5.7 dBi, while with the FSS reflector, the average peak gain is 10.9 dBi.

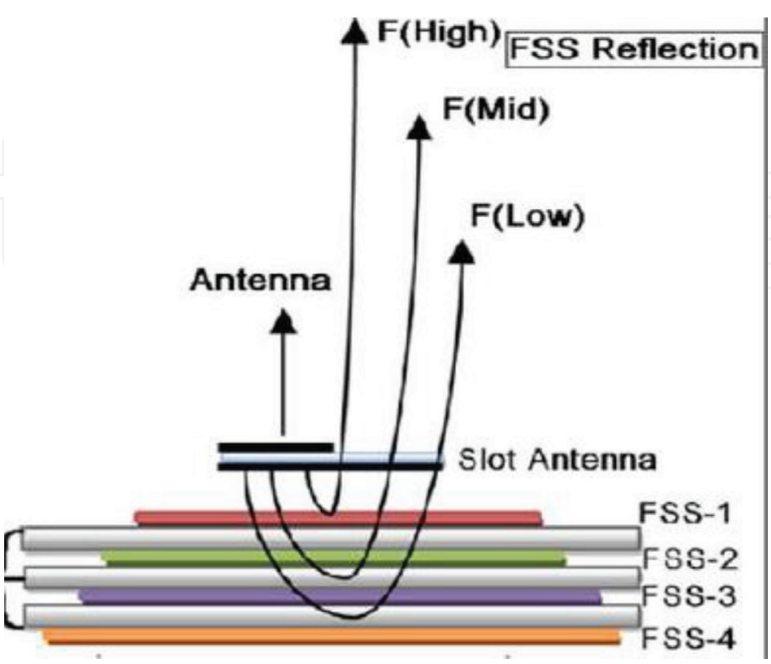


**Figure 3.** Multilayer FSS for constant gain UWB antenna [9].

In [9], a four-layer FSS has been used to form a UWB reflector. The four layers are separated by dielectric layers of thickness of 1.58 mm, and a UWB microstrip slot antenna is placed at a distance of 19 mm above the FSS reflector. With this structure, an average peak gain of 9.3 dB was achieved with an oscillation of ±0.5 dBi, versus an average peak gain of 4 dBi and a variation of ±2 dB of the UWB microstrip slot antenna without the reflector. **Figure 3** illustrates the structure in [9].

## 4. Design of FSS-based reflectors

In this section, we aim to design reflectors to be able to reflect the incident waves over the entire UWB band. A perfect electrical conductor (PEC) plane can be used as a reflector, but its performance cannot be guaranteed over a broadband frequency range as UWB band, especially over the higher frequencies. Frequency selective surfaces can be employed to alleviate this limitation as in [4]. As a result, a grounded FSS will serve as a broadband reflector. Also, this reflector needs to have a reflection coefficient that varies with frequency in a manner that stabilizes the gain of the UWB antennas over the entire operating band. Therefore, a grounded FSS with high resonance frequency is used to achieve these two features. Furthermore, a single-layer UWB stop-band FSS is designed and will be used as a UWB reflector, and its behavior will be compared with that of the other reflectors.

### 4.1. Grounded FSS reflector

An FSS with an array of conductors is fully reflective at resonance frequency where it acts as a metallic sheet, and it remains transparent at other frequencies. This feature of FSS with conductor array can be used to design partial reflector with a desirable reflection coefficient by choosing the location of its resonance frequency.

An FSS of conductor elements, at a high resonance frequency, is mostly transparent with a reflection magnitude that increases with frequency. After that, the transmitted waves can be reflected totally using a PEC ground plane. In this way, the grounded FSS will improve the gain of the used radiator across the entire UWB band with different amount of enhancement; hence, a constant gain can be achieved.

A grounded FSS can also be considered as a grounded dielectric slab loaded with periodic patches, which is similar to a high impedance surface with removed vertical vias. Although removing the vertical vias from HIS mushroom-like structures leads to the disappearing of the EBG, the surface waves can exist over the entire frequency band, and it has little effect on the in-phase reflection feature or AMC feature when the plane wave is normally incident, which is the main interest for our purpose.

Therefore, as a starting point, we used the initial parameters (2), suggested in [10] to analyze EBG ground planes, to design a grounded slab loaded with periodic square shape patches of width W and gap width g between the unit cells, as indicated in **Figure 4**.

$$W = 0.12\ \lambda o, g = 0.02\ \lambda o, hu = 0.04\ \lambda o, \varepsilon r = 2.20 \quad (2)$$

where λo is the wavelength at 7 GHz, which is around the center frequency of the UWB band, and hu is the thickness of the substrate of dielectric constant εr.

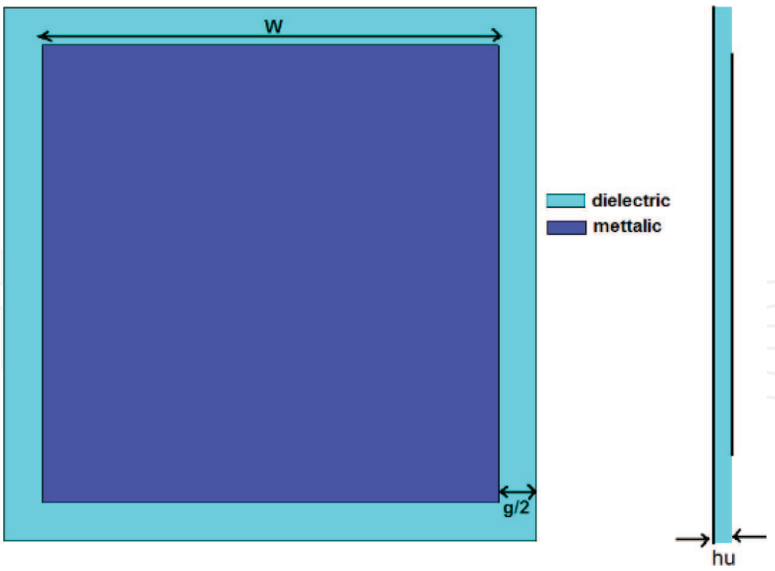


**Figure 4.** Structure of the FSS unit cell.

The dimensions of the unit cell control the width of the band over which the reflection phase varies between −90° and 90°, which can be called the in-phase band [10]. The choice of the used substrate is also an effective factor for enhancing the in-phase band. Therefore, we chose RT/duroid 5880, of a dielectric constant of 1.96, a dielectric loss tangent of 0.0004, and a thickness of hu =3 mm, to obtain a wide in-phase band. For the same purpose, parametric studies of both parameters W and g, around their initial values obtained from (2), were performed, from which the values that give a wide in-phase band centered at 7 GHz are selected. These values are W = 5 mm and g = 0.25 mm.

**Figure 5a** shows the reflection phase of the grounded unit cell with the selected parameters, computed using CST-MWS by considering the "unit cell" boundary conditions and Floquet port. From **Figure 5a**, we can see that broad in-phase band from 5.5 to 8.5 GHz, and AMC feature at 7 GHz are achieved as required.

The reflection magnitude of the unit cell without a ground plane varies, over the UWB band, from 0.3 at the lower frequency to 0.8 at the higher frequency, and it is totally reflective around 45 GHz, as shown in **Figure 5b**. As a result, the reflected amount by the ground plane is unequal, and it is proportionally decreasing with frequency. This unequal amount of transmission is the key feature to achieve a constant gain across the entire UWB, especially if the gain of the used radiator is higher at upper frequencies than it is at lower frequencies, which is the case for most UWB planar antennas.

In [9], the stability of the gain is obtained by allowing the transmission through no backed multilayer FSS, while here it is achieved by only one partially reflective FSS.

### 4.2. Complementary reflector

The operation mechanism of the grounded FSS reflector treated in the last subsection can be realized differently, in a manner that leads to further improvement, by using the complementary technique.

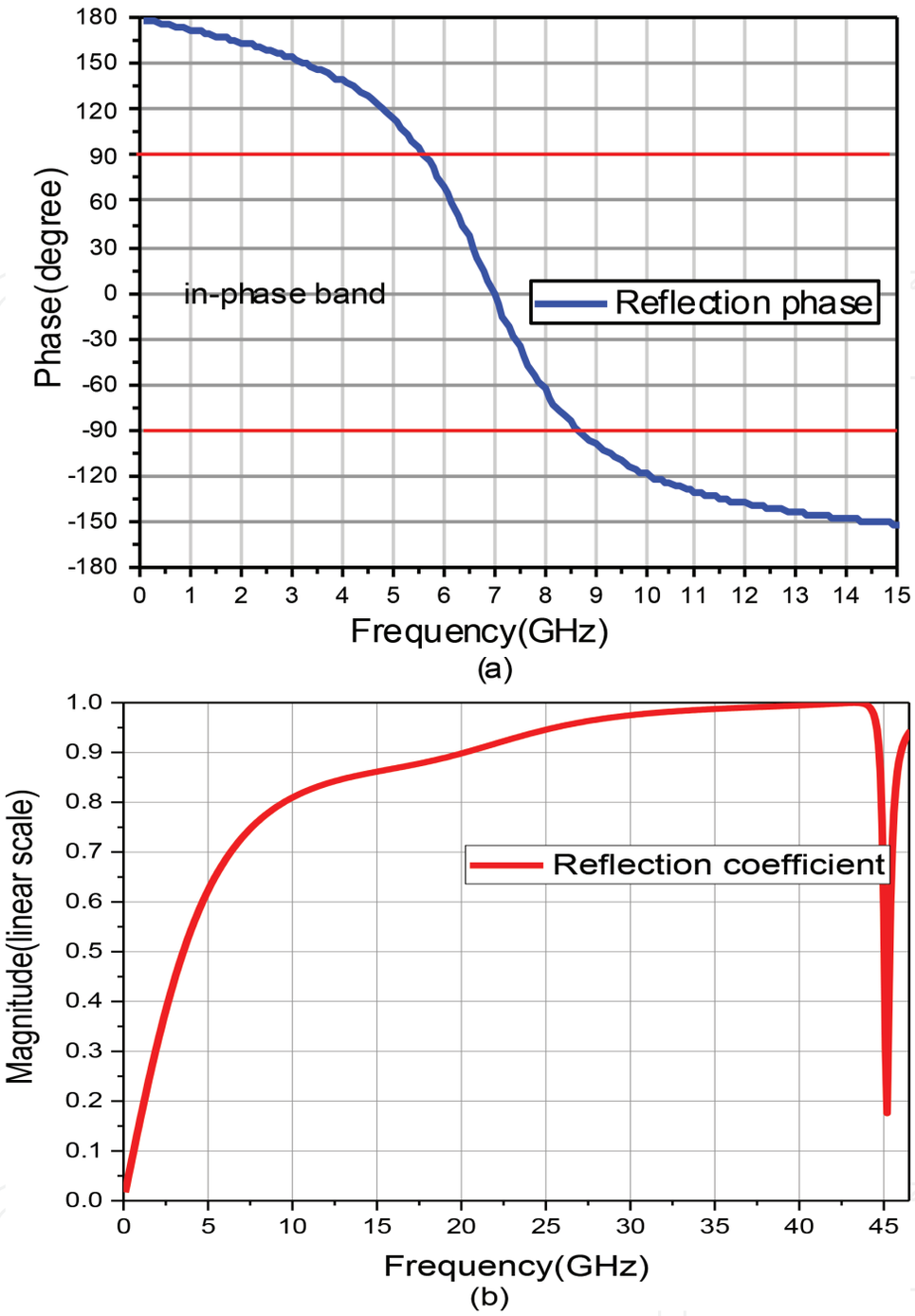


**Figure 5.** Reflection characteristics of FSS. (a) Phase reflection of the grounded FSS with optimized dimensions, (b) reflection magnitude of the FSS without a ground plane.

The complementary structure of the previously used FSS is an array of square slots of width Wc and metallic gap width gc, where Wc and gc have the same values as those of W and g of the grounded FSS. The complementary FSS is printed on a similar substrate to that of the grounded FSS. **Figure 6** shows the structure of the complementary unit cell as in comparison with the grounded one.

This complementary structure will have interchanged S-parameters with the original one according to Babinet's principle. As a result, a reflector with similar behavior as the grounded FSS can be obtained.

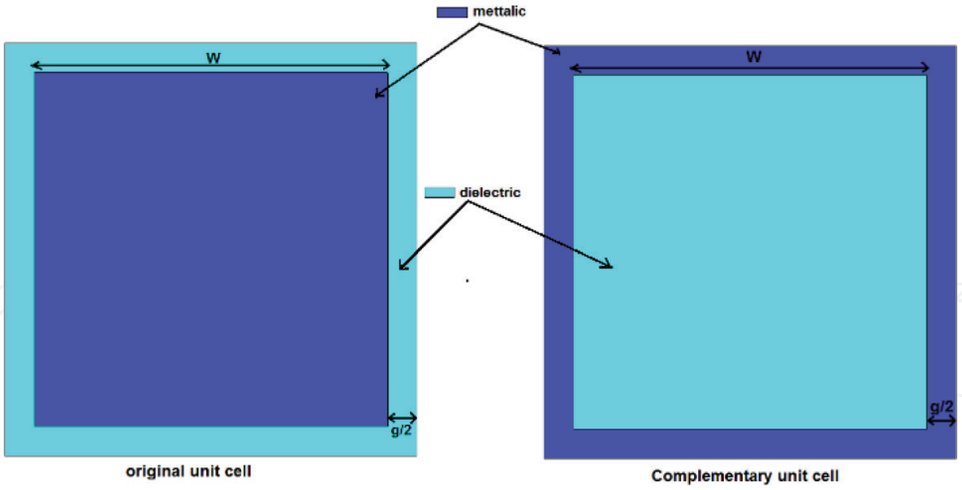


**Figure 6.** Structure of the complementary unit cell in comparison with the original unit cell.

While the ground plane of the grounded FSS reflects the partially transmitted waves through the square conductor unit cells, the complementary FSS operates by partially transmitting the incident waves and reflects most of them with different amount across the frequency band.

As the FSS with aperture unit cells has a high resonance frequency, its reflection magnitude decreases with frequency, which can be clearly seen in **Figure 7**. As a consequence, the amount of the transmission through the FSS will be smaller, at lower frequencies than it is at higher frequencies.

### 4.3. UWB FSS reflector

It has been proved, in Section 3.2 that an FSS with UWB stop-band response can serve as a good UWB reflector when it can provide linearly decreased reflection phase over the UWB band. The proposed UWB FSS offers UWB stop-band response and linearly decreased reflection phase across the UWB band; hence, it owns the ability to serve as a UWB reflector. To design an FSS with UWB stop-band response, we follow the idea of merging two structures with the ability to resonate at adjacent frequencies while their dimensions and geometries can allow them to be integrated together. So the first step is to find such structures. Loop types resonate when their circumference is approximately a wavelength that makes them a good choice for our purpose especially that their geometries are flexible enough to be combined with each other or even with other types.

The square loop resonates when its four sides' length takes a quarter of the wavelength as its value and the circular ring resonates with a diameter of $D = \frac{\lambda}{\pi}$. Hence, the square loop resonates with a total length smaller than that of the circular ring. Combining these two structures leads to the construction of a dual-band response where the lower resonance frequency is dictated by the square loop, and the higher frequency is controlled by the circular ring. The pass-band between the two resonance frequencies is governed by the distance separating the two structures. As made known in the previous section, the dielectric substrate, over which the FSS is printed, plays a vital role in determining the FSS characteristics, especially its size at resonance. Therefore, the choice of the FSS dielectric substrate can be beneficial in miniaturizing unit cell size, as a high dielectric constant substrate can reduce the size of the unit cell

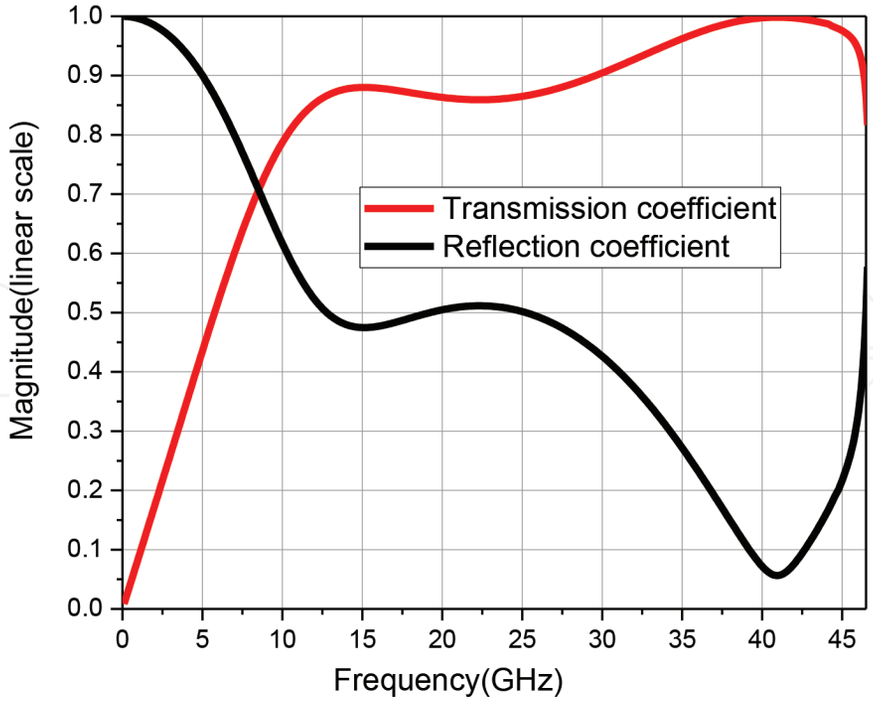


**Figure 7.** Reflection and transmission magnitude of the complementary unit cell.

by a factor of $1/\sqrt{(\epsilon_r + 1)/2}$ compared with a unit cell printed on a foam substrate (with dielectric constant equals unity). Consequently, RT/duroid 6010.2LM with a dielectric constant of 10.2, a tangent loss of 0.0023, and a thickness of 0.625 mm has been chosen as the dielectric substrate over which the proposed FSSs are printed.

After choosing the geometries of the FSS unit cells that serve our purpose, we need to study these unit cells using a 3D simulator for a further investigation of their behavior and how they react to the parameter variations.

It is important to mention that all the graphs presented in the next subsections are for a normal incidence. Due to the symmetry of all these FSSs, the obtained responses under TE-polarization are similar to those obtained under TM-polarization. Hence, for the sake of brevity, only the responses obtained under TE-polarization is presented.

We have studied the effects of varying the parameters of the square and circular ring unit cells, more details can be found in [11, 12], from which the design guides can be derived. Now, we shall study the effect of combining them. Although they respond to the variation of their parameters in similar ways, the square loop resonates at smaller dimensions compared to the circular ring. Consequently, for a miniaturized unit cell, the circular ring should be integrated into the square loop as depicted in **Figure 8**.

To visualize the effect of the spacing between the two elements, only "$R_{out}$" is varied while all the other parameters are kept constant, and the transmission coefficient is calculated for each case. The results of this study are illustrated in **Figure 9**.

As "$R_{out}$" increases, the resonance frequency of the circular ring decreases, approaching that of the square ring. Thus, the band-pass between the two resonance frequencies gets narrower while merging both structures results in a UWB band-stop response.

http://dx.doi.org/10.5772/intechopen.79888

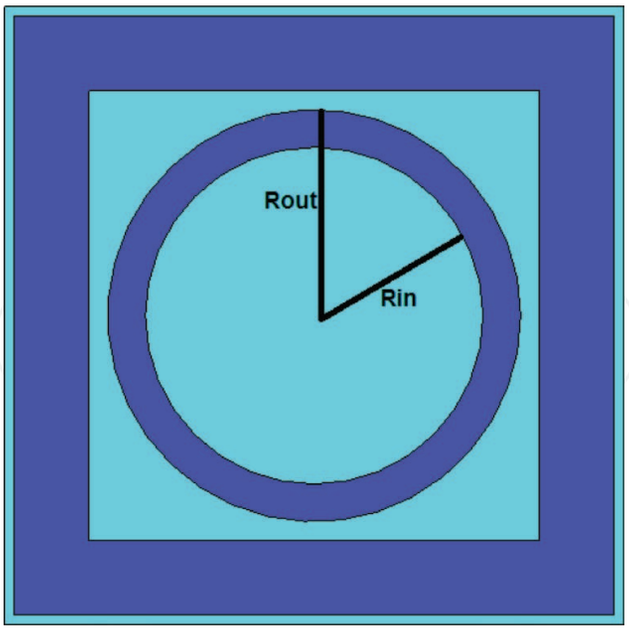


**Figure 8.** Circular ring inserted within square loop unit cell.

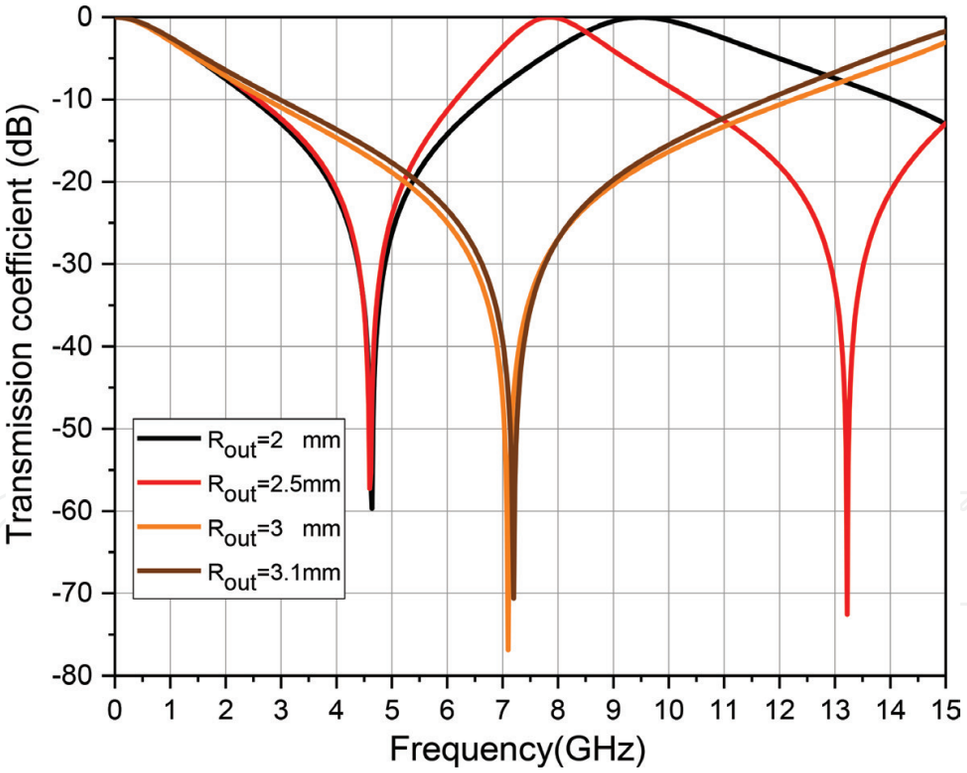


**Figure 9.** Parametric study of transmission coefficient for different values of $R_{out}$.

The results of the previous studies can help deliver a design guide of the combined UWB FSS as follows:

- The square loop resonates at smaller dimensions compared to the circular ring. As a result, the circular ring should be integrated into the square loop to obtain a miniaturized unit cell.

- The lower edge of the stop-band of an FSS, consisting of square loop unit cells, is governed by the external length of the square loop and the gap width between the unit cells; hence, they should be chosen so that the desired lower edge of the stop-band is obtained.
- After fixing the external length along with the gap width, for a desired lower edge of the stop-band, the width of the band as well as the resonance frequency can be adjusted through the variation of the internal length.
- The two element structures can be merged to obtain a UWB band-stop response.
- The outer radius of the circular ring controls the lower edge of its operating band but, in here, it also controls the spacing between the combined elements.
- The outer diameter of the circular ring should be equal or slightly superior to that of the internal length of the square loop for them to be merged.
- The inner radius of the circular ring can be used to set the desired overall upper frequency.

Taking into consideration the entire design guide mentioned above, the geometry of the proposed UWB stop-band FSS unit cell and its final parameters are illustrated in **Figure 10** and **Table 1**, respectively. It is worth mentioning that the above design guide can be generalized to implement UWB FSSs with combined elements of different geometries.

**Figure 11** indicates the computed reflection and transmission coefficients of the proposed FSS. These graphs prove the ability of the proposed UWB FSS to act as a stop-band filter over a wide-band from 3 to 12 GHz, which includes the entire UWB band, with a reflection magnitude of 0 dB and a transmission magnitude less than -10 dB. At the main resonance frequency, around 7 GHz, the transmission magnitude becomes less than −75 dB. The computed

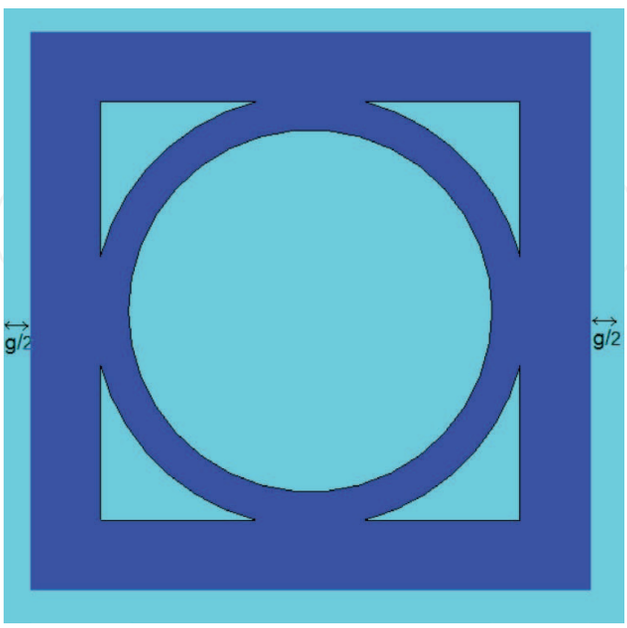


**Figure 10.** Structure of the proposed unit cell.

| $L_{out}$ | $L_{in}$ | $R_{out}$ | $R_{in}$ | G |
|---|---|---|---|---|
| 8 mm | 6 mm | 3.1 mm | 2.5 mm | 0.25 mm |

**Table 1.** Final dimensions of the proposed FSS unit cell.

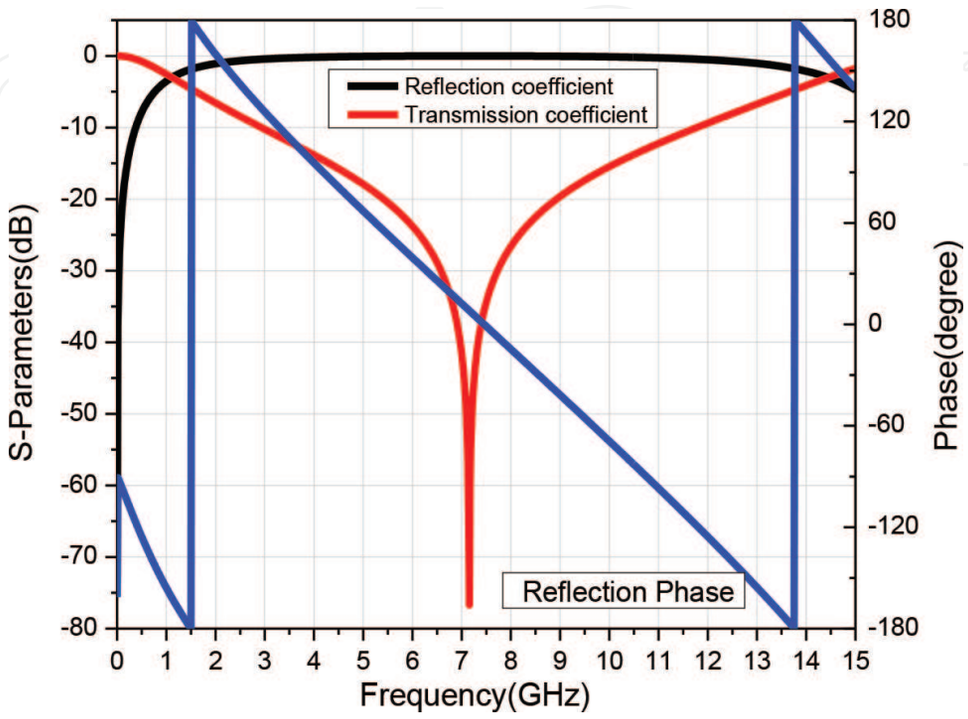


**Figure 11.** Reflection and transmission coefficients of the proposed FSS.

reflection phase of the FSS decreases linearly with frequency and has zero value around 7 GHz, where the transmission magnitude takes its lowest value.

The linearity of the reflection phase of the proposed FSS is satisfied across the whole band from 2 to 14 GHz. This special feature extends the recommended applications of our proposed FSS to include a variety of systems where a linearly decreasing phase is required.

## 5. Reflectors with UWB radiator

For better evaluation of the proposed design concept, a UWB planar antenna is used as a radiator. The original design of this UWB planar antenna has been proposed in [13]. It is a CPW-fed circular disc antenna printed on a dielectric substrate as shown in **Figure 12**. In here, the employed substrate is RO4003C with a dielectric constant of 3.38, a dielectric tangent loss of 0.0027, and a thickness of 0.508. The dimensions of the CPW line are $w_f$ = 3 mm and $s_f$ = 0.28, where the former is the width of the main line, the latter is the gap between the main line of the CPW and the ground plane, and 's' is the slot gap between the circular patch and the ground plane.

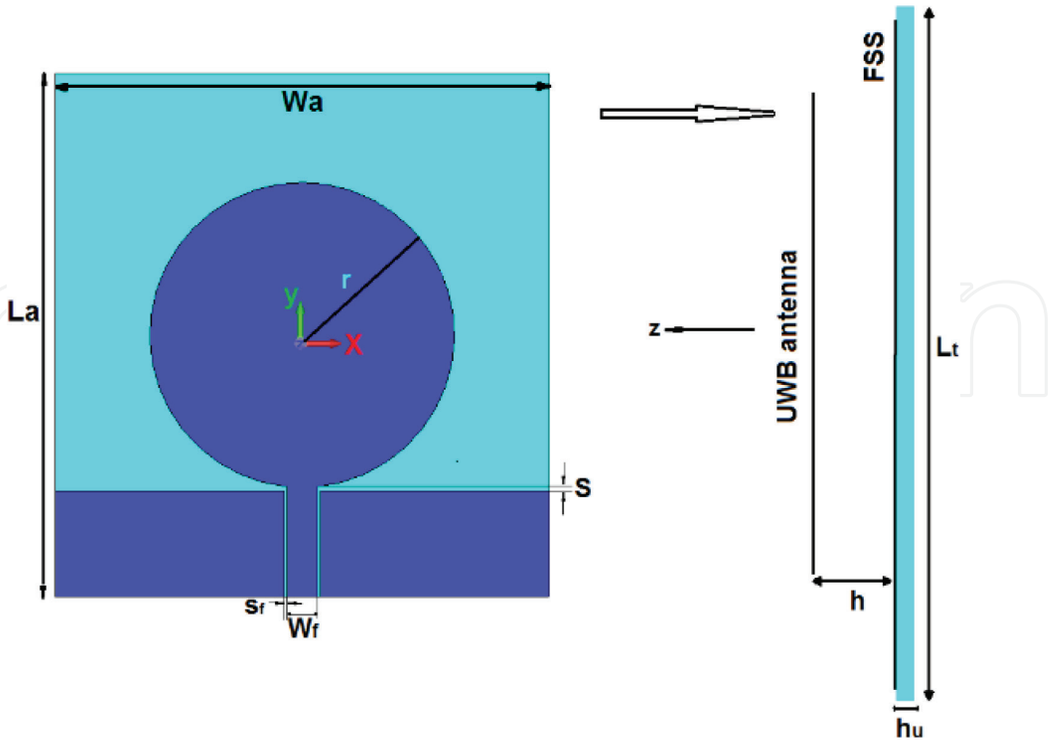


**Figure 12.** Structures of the used UWB antenna and the proposed structure.

The dimensions of the used radiator are illustrated in **Table 2**. The radiator is located at a distance "h" above the grounded FSS, complementary FSS, and UWB FSS, as indicated in **Figure 12**.

Many parameters affect the overall performance of the combined structures such as the distance between the antenna and the reflector and the number of the unit cells that constitute the latter.

The parameters of the grounded reflector include W, g and the number of cells n1 that is constituted of, along with the distance "h1" were optimized in terms of maximizing the operating band and minimizing the peak gain variation over frequency. Thus, the optimized values that give the best performance were selected, and they are given in **Table 2**. The dimensions of the complementary reflector are the same as those of grounded reflector.

The optimization of the grounded reflector parameters reveals that the best results are obtained when the length of the square patches is very small (W = 3 mm), which results in a higher resonance frequency compared with that associated with the initial value W = 5 mm

| W | g | La = Wa | R | S | h1 | n1 |
|---|---|---|---|---|---|---|
| 3 | 0.25 | 50 | 14.5 | 0.35 | 15.5 | 24 |

**Table 2.** Optimized values of the parameters of grounded and complementary reflectors along with the dimensions of the UWB radiator (in mm).

and hence, a less amount of transmission through the FSS. Moreover, it can be noted that for stabilizing the gain, the in-phase reflection should not necessarily be at the center frequency of the UWB band and that its location depends on the scattered waves from the ends of the reflectors and the different factors that set the added phase through the distance between the radiator and the reflector, which is a function of frequency.

Regarding the UWB reflector, the same dimensions of its unit cells, found in **Table 1**, were kept and parametric studies were performed to choose the best values of its distance from the radiator and the number of cells. The results of these studies are shown next.

First, the effect of the distance between the radiator and the UWB reflector on the operating band is studied through a parametric study of the reflection coefficient of the antenna for different values of "h2," as shown in **Figure 13a**. As expected, the FSS affects the matching band of the radiator as when "h2" increases, the bandwidth of the antenna increases. Furthermore, the influence of this parameter on the radiation behavior of the antenna is clearly illustrated in **Figure 13b** where the peak gain, across UWB band, is computed for different values of "h2." This points out that the gain changes differently over frequency, which can be explained by the fact that the phase shift added by h2 is a function of frequency.

As a summary, we can derive that the operating band, stability, and the value of the maximum gain of the antenna are highly dependent on how far the radiator is from the reflector.

The size of the FSS determines the overall size of the antenna. Therefore, a deep study of the effects of the installed FSS size on the provided performance was performed. The results of this study are shown in **Figure 14**. **Figure 14a** contains the reflection coefficient of the antenna for different numbers of cells (n2), which models the size of the FSS, revealing that the matching band of the antenna is mainly affected by the part of the FSS that is located directly under the radiator. In other words, when FSS dimensions exceed those of the radiator, the bandwidth of the antenna becomes independent of the FSS size.

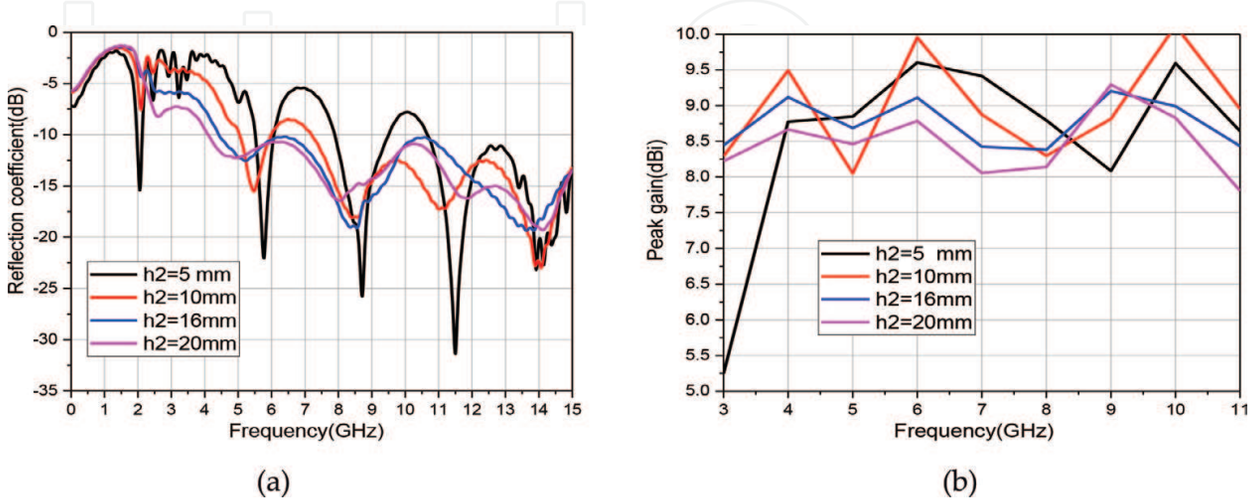


**Figure 13.** Parametric studies of the parameter h2. (a) Reflection coefficient, (b) peak gain.

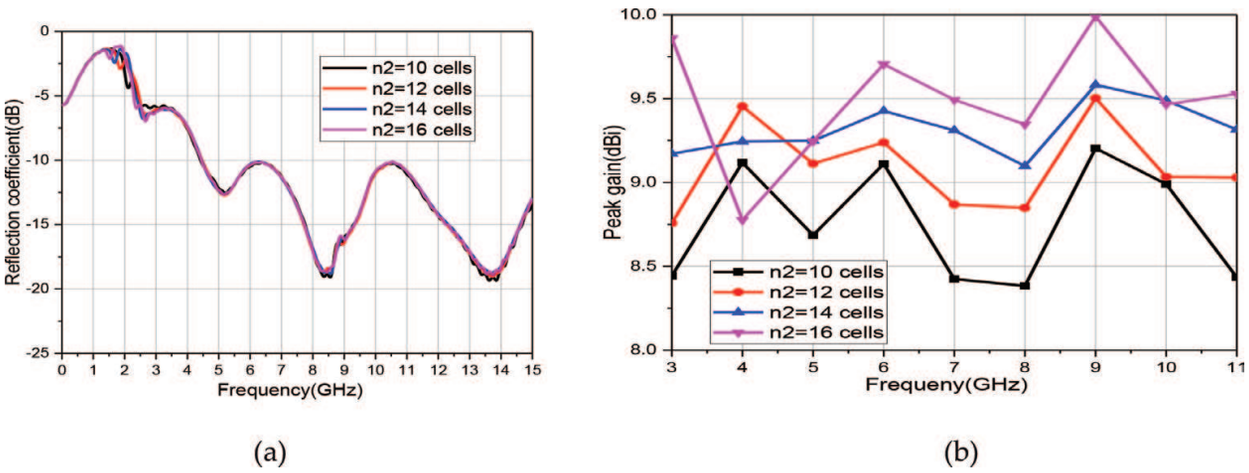


**Figure 14.** Parametric studies of different values of number of cells n2 of UWB reflector. (a) Reflection coefficient, (b) peak gain.

The reflective behavior of the UWB FSS is computed by considering infinite FSS dimensions, which cannot be realized in practice where finite size structures are required. However, with a large number of cells, infinite dimensions can be approximated. Nonetheless, the size of the FSS affects mainly the radiation behavior of the antenna, which is shown in **Figure 14b** through a parametric study of the antenna peak gain, illustrating that as the number of cells increases, the gain also increases over the entire UWB band. A smaller reflector can be used but at the expense of the achieved gain.

Therefore, we chose the value of "h2" that gives a wide operating band and the number of cells that is associated with high gain and minimum gain variation across the achieved band. Finally, the parameters of the structure were optimized, using CST-MWS, to achieve UWB matching band with a quasi-constant gain. The final dimensions of the UWB FSS reflector are indicated in **Table 3**.

### 5.1. Numerical and experimental results

The three proposed reflectors, with the optimized dimensions, along with the used radiator were fabricated and their photographs are shown in **Figure 15**.

In the three cases, the reflection coefficient of the UWB antenna and its peak gain and radiation patterns were computed numerically and measured.

It is worth mentioning that the peak gain is chosen for the evaluation rather than the gain at a specific direction because the radiation behavior of the used radiator is unstable, by nature, meaning that the direction of its mean radiation varies with frequency. Hence, the peak gain

| Lout | Lin | G | n2 | h2 |
|---|---|---|---|---|
| 8 | 6 | 0.25 | 14 | 16 |

**Table 3.** Final dimensions of the UWB FSS reflector used with the UWB radiator with single polarization (mm).

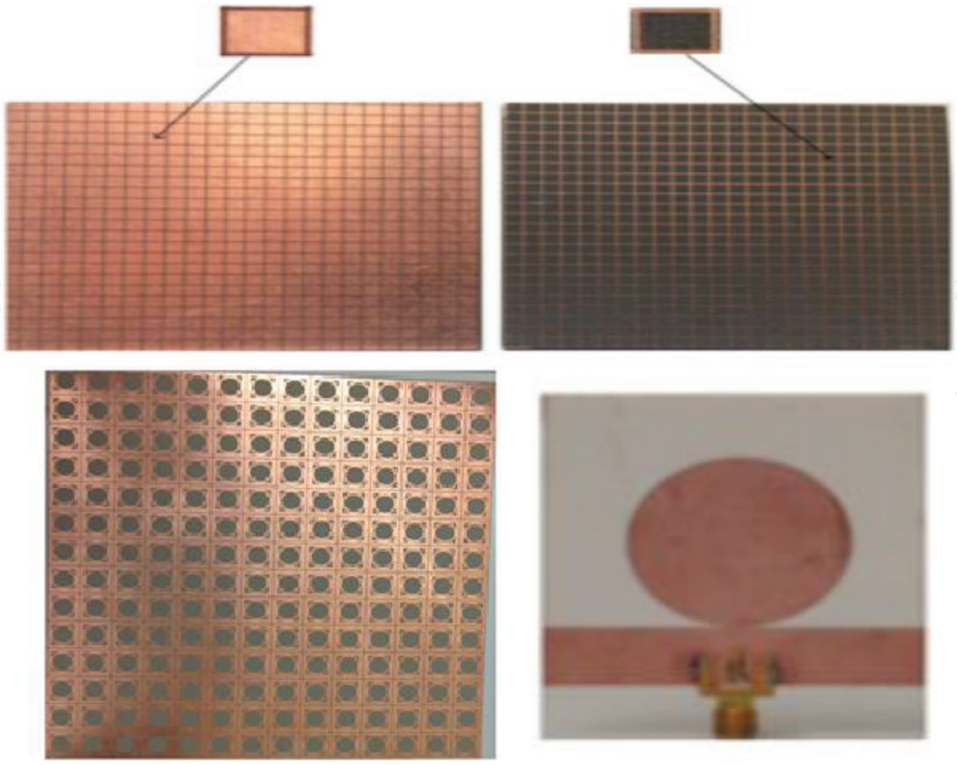

**Figure 15.** Fabricated prototypes.

will show, in more general way, the ability of the proposed reflectors to enhance the gain over the entire UWB band.

**Figures 16–19** illustrate the final results of the simulation and measurement of the proposed designs. **Figure 16** shows the reflection coefficient of the UWB antenna mounted above the proposed reflectors, while **Figure 17** indicates the simulated peak gain over frequency, which is

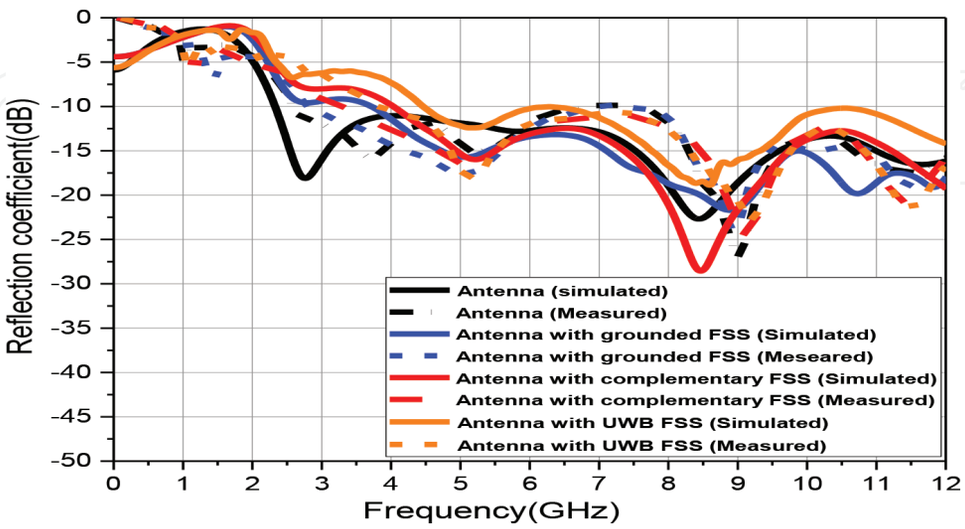


**Figure 16.** Reflection coefficient of UWB antenna with and without reflectors.

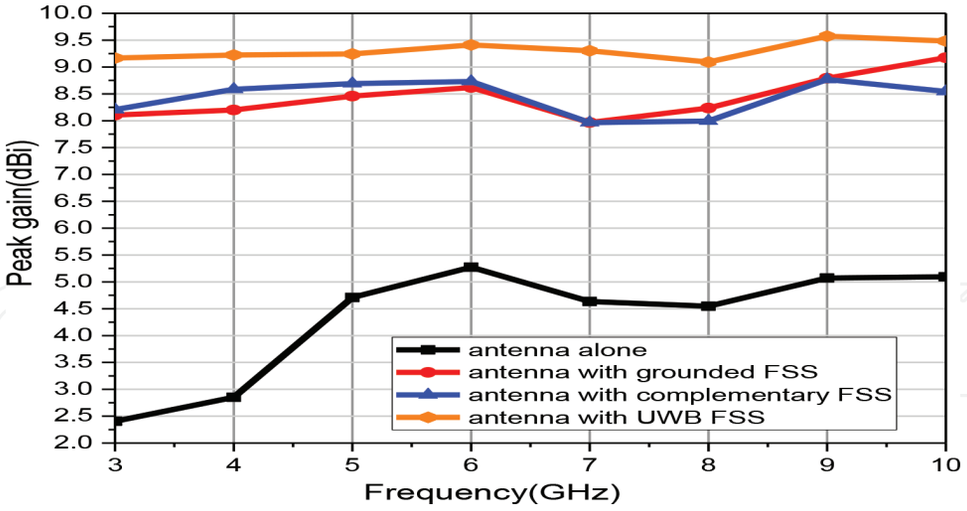


**Figure 17.** Peak gain of the UWB antenna with and without reflectors.

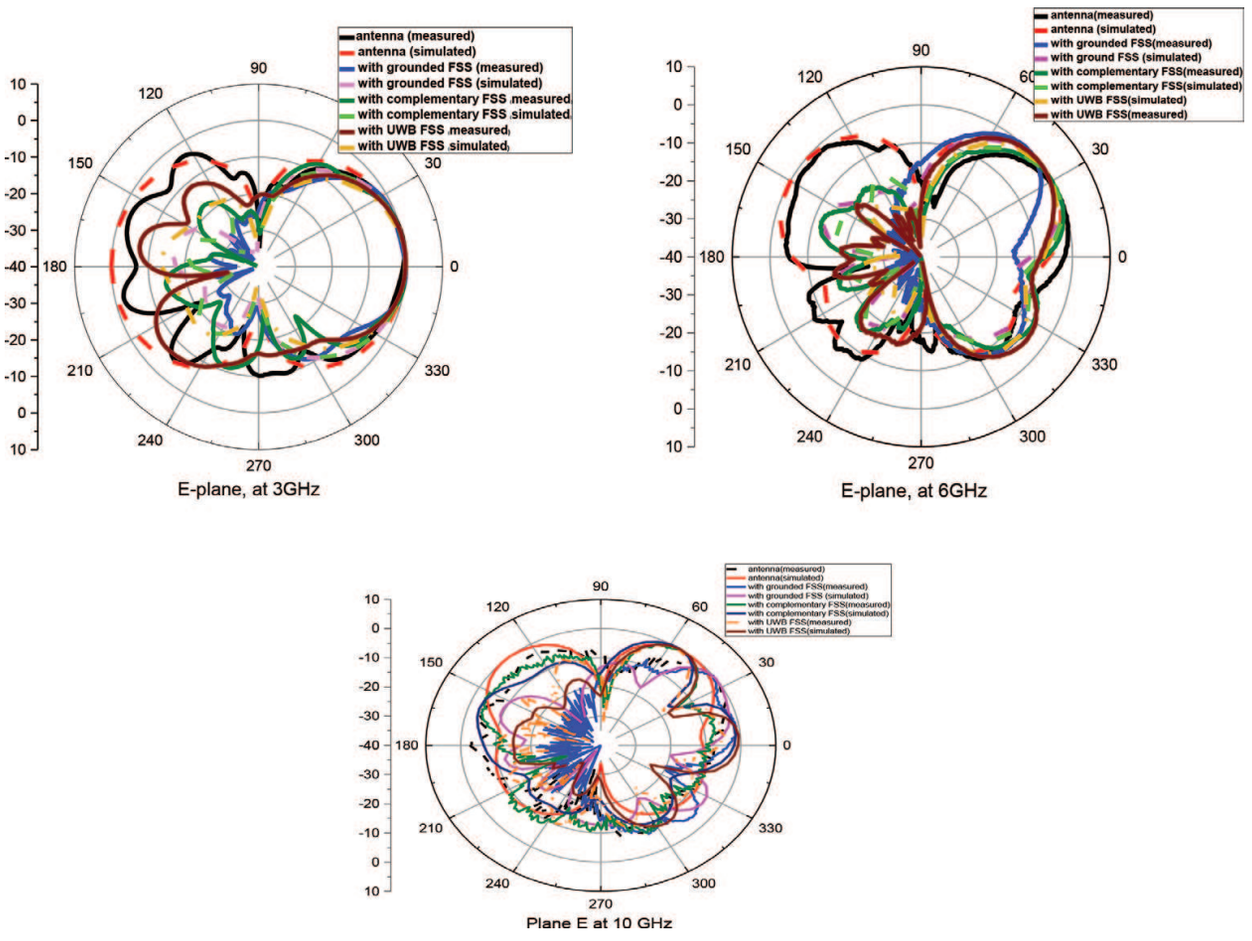


**Figure 18.** Radiation patterns in E-plane (YZ) at different frequencies.

extracted from the 3D radiation patterns calculated at each frequency. The direction of the maximum radiation can be shown clearer through the 2D radiation patterns, which will be shown later on. These figures also contain the corresponding results of the UWB antenna without reflectors to allow a clear visualization of the achieved improvement owing to the reflectors.

http://dx.doi.org/10.5772/intechopen.79888

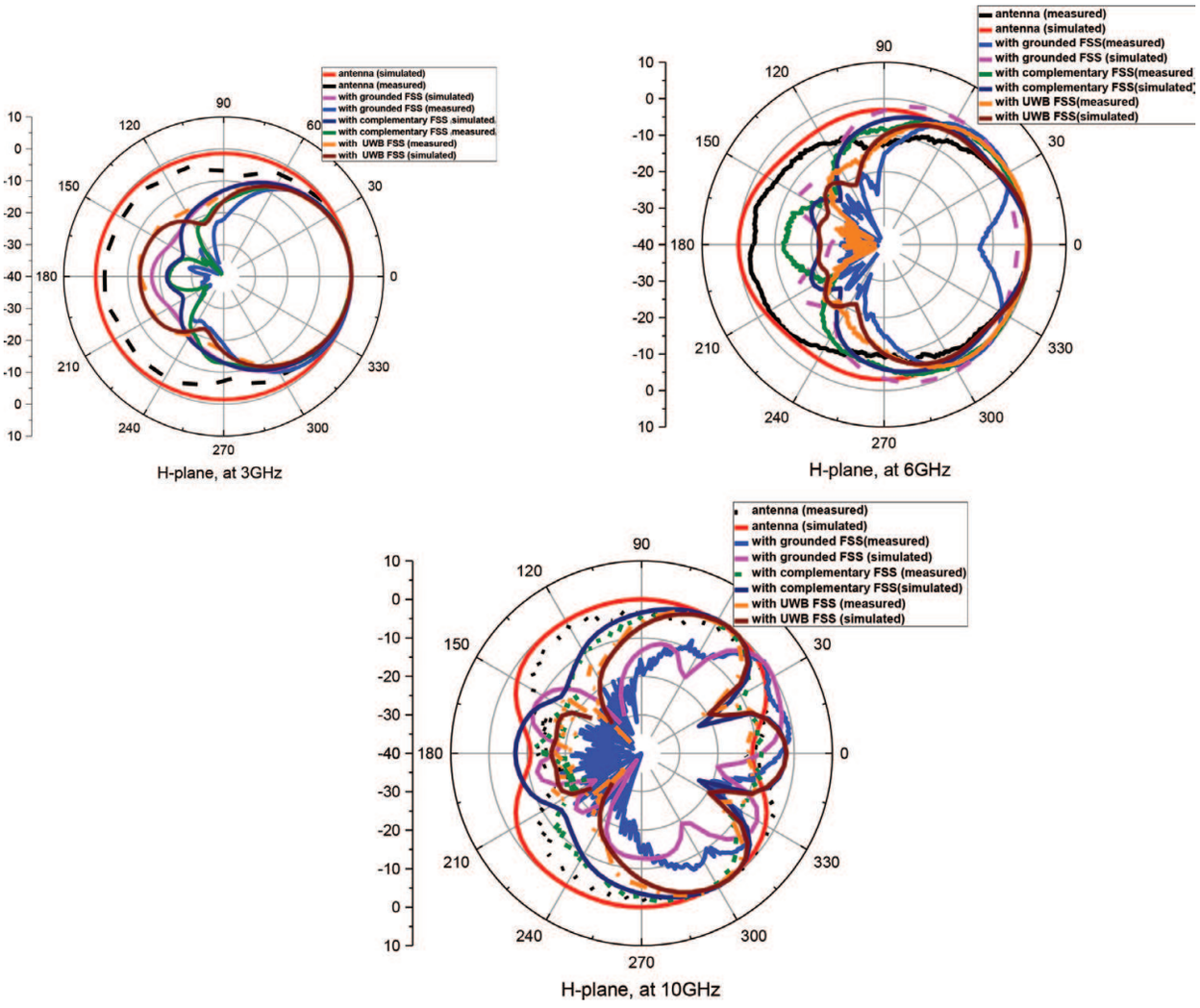


**Figure 19.** Radiation patterns in H-plane (XZ) at different frequencies.

These results prove that the provident choice of the different dimensions gives antennas with operating band covering the FCC authorized band from 3.1 to 10.6 GHz and an average peak gain of 8.5 dBi with a maximum variation of 0.6 dBi for the first two reflectors.

The comparison between the reflection coefficient of the radiator installed at the chosen value of h2 (h2 = 16 mm) from the UWB FSS reflector and that of the radiator alone without reflector reveals that at this height the FSS affects the matching level of the antenna, especially over the lower part of the UWB band. Regarding the gain, **Figure 17** illustrates the maximum gain of UWB antenna with and without UWB FSS. It is evident that the antenna gain is enhanced across the UWB band as a result of using the UWB FSS. The amount of enhancement varies, across the band, from 6 dBi at 3 GHz to 3.5 dBi at 10 GHz, which led to a quasi-constant gain with a maximum variation in gain of 0.7 dBi. As a result, a planar UWB antenna with enhanced quasi-constant gain is obtained.

It can also be noticed that the antenna above the three reflectors shows a similar behavior, except small differences, over the UWB band. The simulation and measurement results show an acceptable agreement.

The radiation patterns simulated and measured in E and H planes, which correspond to (YZ) and (XZ) as indicated in **Figures 18** and **19**, respectively, show the good effects of the reflectors on the radiation behavior of the antenna and confirm the gain enhancement, which is basically because of the back radiation reduction.

At higher frequencies, the radiation patterns start to be distorted with multiple side lobes due to the distortion and mean radiation tilt of the used radiator, which is a common behavior of UWB monopole antennas. However, the proposed reflectors have the ability to stabilize the peak gain despite the radiation distortion at higher frequencies, suggesting that using a more stable radiator can lead to constant and stable radiation. By taking into account their particularity and by following the proper design methodology, similar results can be obtained using other UWB monopole antennas as radiators.

Each one of the proposed reflectors has a special operation mechanism. The first one uses the ground plane to reflect the incident waves transmitted through the FSS, where the main role of the latter is to stabilize the gain by controlling the transmission over UWB band. This reflector occupies both sides of the dielectric substrate and because of the ground plane, it is fully reflective at all frequencies even those outside the UWB band. This can be inconvenient for the nearby radiators as their radiation will be blocked even if they are not sources of interference.

On the other hand, the complementary FSS, which covers only one side of the dielectric substrate, has a lower effect on the nearby radiators that operate outside the UWB band. Meanwhile, the mounted radiator will not be completely isolated from surroundings.

The third reflector gathers the best characteristics of the two previously mentioned reflectors as its structure occupies a single side of the dielectric substrate and it is fully reflective over UWB band. Hence, it will isolate the radiator from surroundings without being an obstacle for the out of UWB band radiators because it is transparent outside UWB band.

Due to the superiority that UWB FSS reflector shows, it will be used to design UWB FSS-based antenna.

## 6. UWB FSS-based antenna

The plane wave analysis is the most common way to study and emphasize the performance of frequency selective surfaces where the incident waves are considered planar with angles of incidence around the normal on the FSS plane. Although this analysis method is useful for most of the applications that use FSSs as radomes and space filters, it is not that much useful when the FSSs are to be integrated into the near-field zone of an antenna.

However, several references used the plane wave approach to give a design guide for the FSS-based antennas [8, 14]. On the other hand, Ref. [15] showed that the interactions between antennas and FSSs could not be sufficiently addressed without a full-wave analysis of the actual antenna structure in the presence of the FSS.

Therefore, instead of using the FSS to enhance the bandwidth of narrowband radiators as in [15] or using FSS-based reflectors to improve the gain of predesigned UWB radiators as in [8, 9]

and the previous section, we follow an approach that gathers the best of all, where the UWB radiator along with the FSS is designed together to achieve UWB, low profile, and high quasi-constant gain antenna. In the previous section, the study of effects of "h2" on the matching band of the antenna showed that as this parameter increases, the bandwidth of the antenna increases. However, one should pay attention to the fact that the parameter "h2" sets the profile of the antenna and hence, a minimum value of this parameter is needed to achieve a low profile.

Therefore, we set "h2" to be 10 mm, which is $\frac{\lambda}{10}$ at the lower frequency of UWB band, instead of 16 mm as in the previous section. Then, the new current distribution, over the structure of

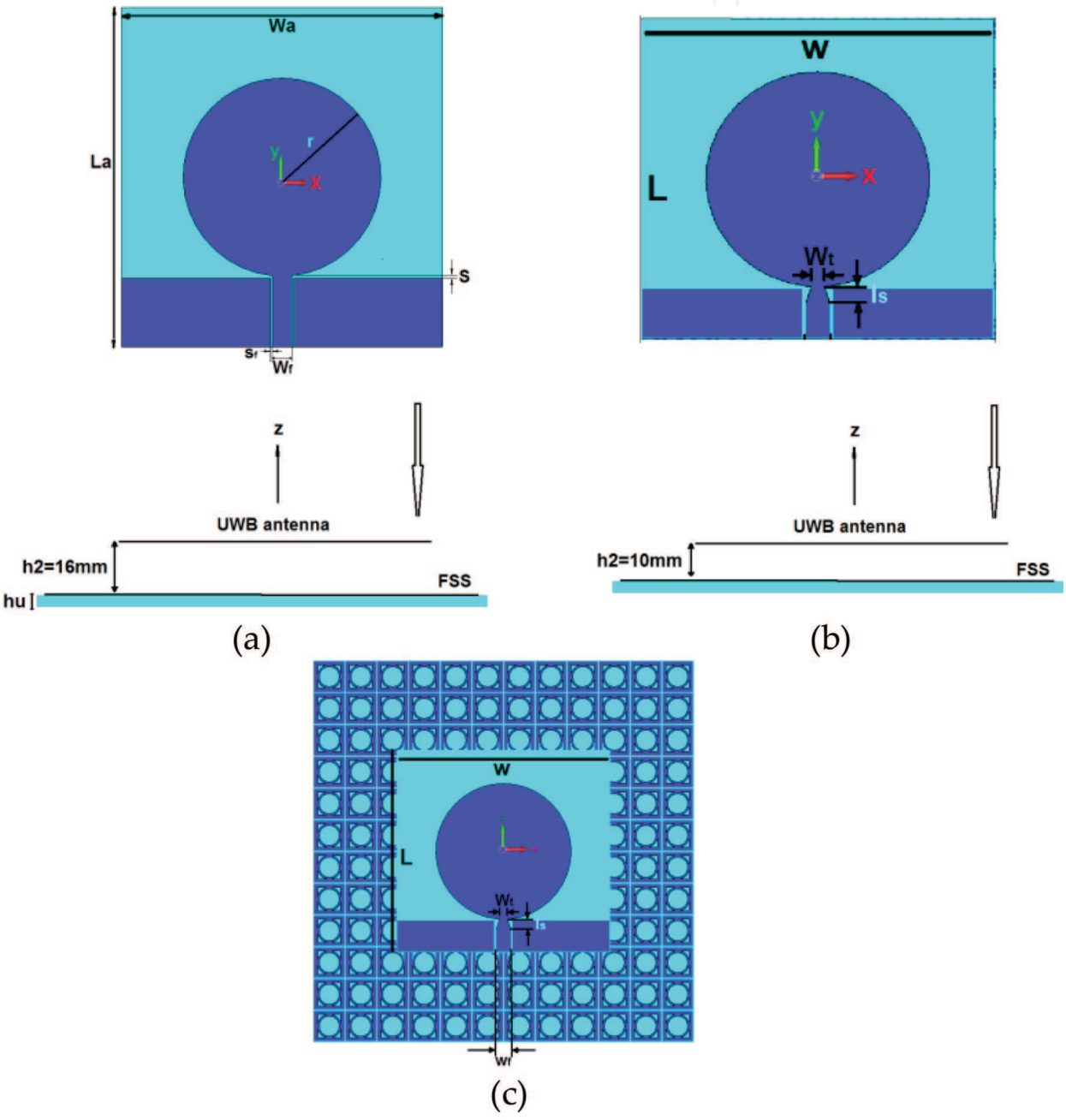


**Figure 20.** Proposed structure of UWB FSS-based antenna. (a) UWB antenna above UWB reflector, (b) UWB FSS-based antenna, (c) UWB FSS-based antenna (front view).

the radiator, imposed by the integration of the FSS was studied and analyzed. The previous analysis of the effect of the reflector size on the matching band of the antenna revealed that the matching band of the antenna is mainly affected by the part of the FSS that is located directly under the source. Consequently, to reduce the time of simulation, we used an FSS consisting of only 8*8 cells during the analysis process to achieve a wide operating band. Subsequently, the radiator was designed to have a wide matching band, and the reflector was designed for high and stable gain. Hence, the parameters of both structures were modified.

The structure of the proposed FSS-based antenna is illustrated in **Figure 20**. The feeding CPW line was tapered and its new parameters are defined in **Figure 20b**.

The modification of the feeding line is necessary to compensate some of the effects of the FSS on the matching band of the source antenna, especially that the tapered area has the most control on the matching band of the antenna due to the high current distribution around this area. This fact can be noted in **Figure 21** where the current distributions over the structure of the initial radiator, the initial radiator at distance 10 mm from FSS with 8*8 cells, and the redesigned radiator with FSS of the same number of cells are shown at 4 GHz. The current distributions are studied at 4 GHz because an impedance mismatch appears at this frequency when the FSS is located at 10 mm from the initial radiator.

Tapering the CPW feeding line and changing the dimensions of the structure lead to the redistribution of the current in a similar manner to that of the antenna without FSS. Also, the current distribution over the FSS is weaker around the redesigned antenna compared with that over the FSS located at 10 mm from the initial antenna.

All the main parameters that control the matching band of the monopole antenna, such as r, w, s, the new feeding dimensions, as well as the dimensions of the FSS unit cells were optimized using CST-MWS.

After finding the parameters of the radiator that give the best performance, the number of cells was parametrically studied, as shown in **Figure 22**, to select the number of cells that gives a high gain with a minimum variation through the operating band. The final optimized dimensions of the proposed antenna are given in **Table 4**.

### 6.1. Final results of FSS-based antenna

**Figure 23** indicates the computed reflection coefficient of the proposed antenna, which shows that a reflection magnitude inferior to −10 dB is achieved along the band from 3.5 to 10.6 GHz. This matching band is obtained for overall profile thickness of 10 mm, which is around $\lambda/10$ at the lower operating frequency, which is wider than that achieved in previous section though the latter has a higher profile of 16 mm.

Regarding the radiation behavior, the peak gain of the proposed antenna and that of previous section, across the frequency, are indicated in **Figure 24**. It is clear that the proposed antenna gain is higher, over higher frequencies of the UWB band than that of the antenna with FSS reflector of the previous section, and it is lower over lower frequencies of UWB band. This is due to the size of the FSS chosen that is smaller in the latter case. However, a quasi-constant gain with a maximum variation of 0.7 dBi across the UWB band is still provided.

http://dx.doi.org/10.5772/intechopen.79888

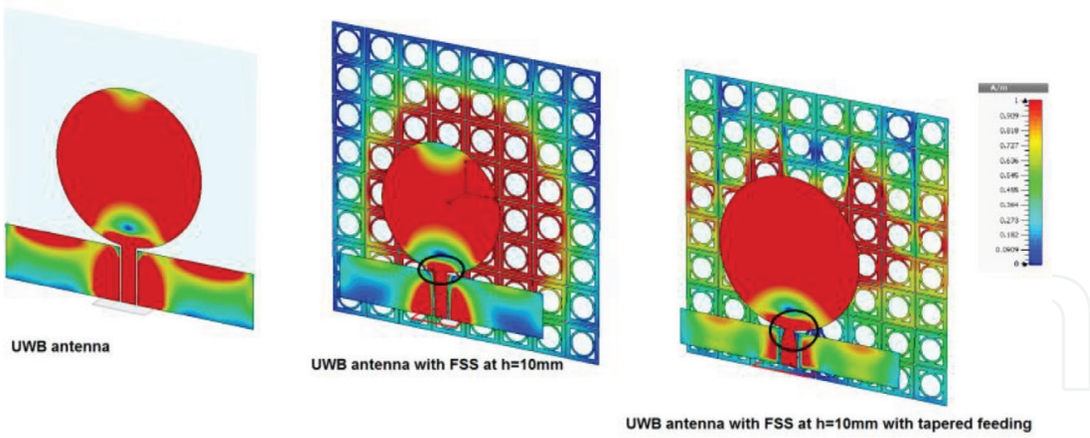


**Figure 21.** Surface current distribution at 4 GHz.

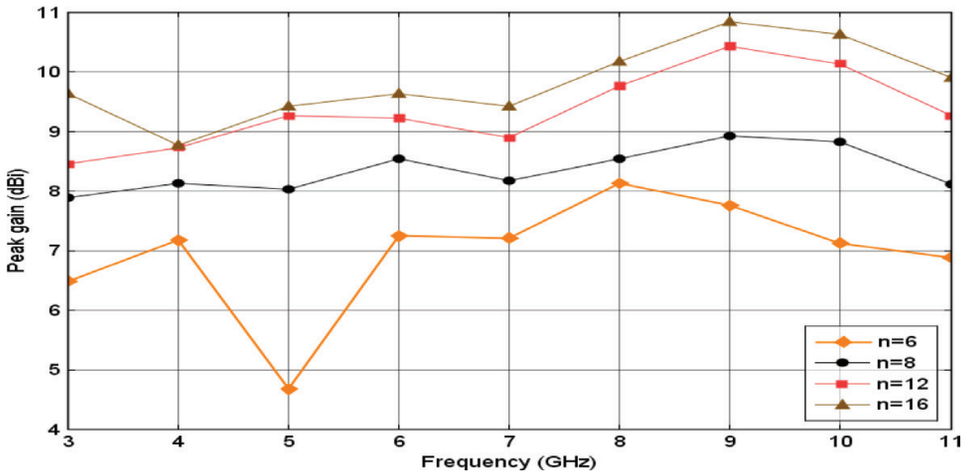


**Figure 22.** Gain for different numbers of cells.

| $L_{out}$ | $L_{in}$ | $R_{out}$ | $R_{in}$ | G | L | W | R | Wt | Hs | N | h2 |
|---|---|---|---|---|---|---|---|---|---|---|---|
| 8 | 6 | 3.1 | 2.5 | 0.25 | 52 | 55 | 17.5 | 2 | 3 | 12*12 | 10 |

**Table 4.** Dimensions of the proposed FSS-based antenna (in mm).

Different factors such as the linearly decreasing reflection phase of the proposed FSS and the small distance between the FSS and the radiator, which cannot be obtained using a flat metallic reflector, contribute in achieving the reached high quasi-constant gain. As a result, a low profile planar UWB antenna with enhanced quasi-constant gain is obtained.

It should be mentioned that the proposed FSS reflectors through this chapter can be integrated with other UWB antennas to achieve further features such as reported in [16, 17], where a UWB dual-polarized antenna [18] was used as radiator to develop UWB FSS-based antennas with diversity operation.

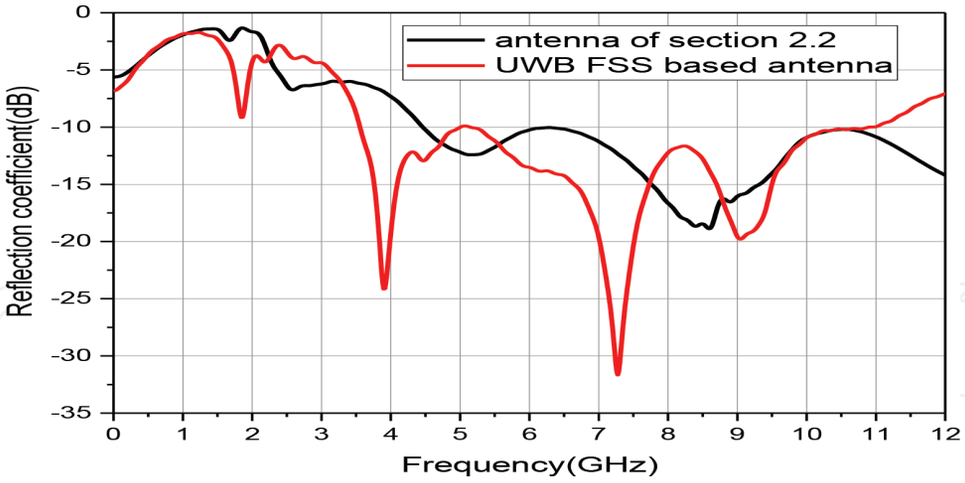


**Figure 23.** Reflection coefficient of the proposed antenna and that proposed in the previous section (UWB antenna with UWB FSS).

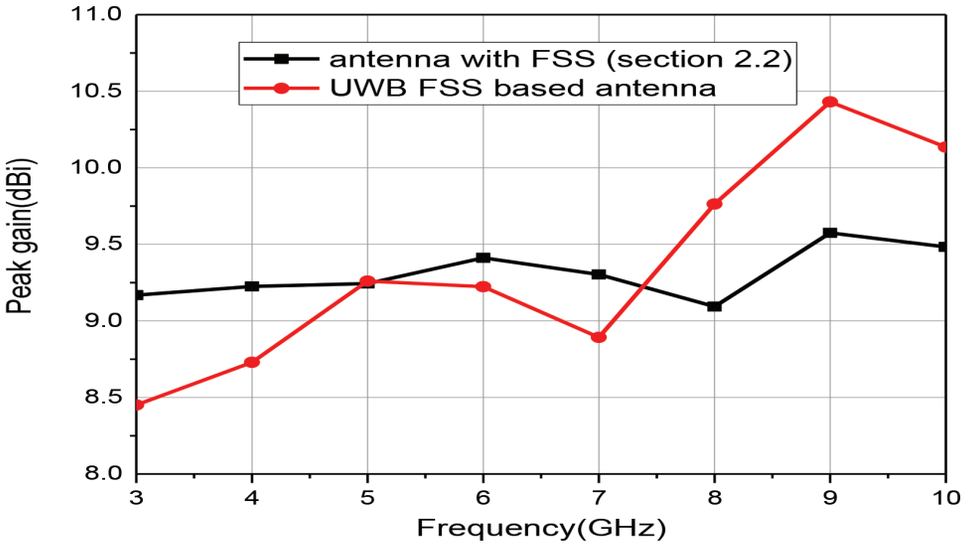


**Figure 24.** Peak gain of the proposed antenna and the one proposed in the previous section (UWB antenna with UWB FSS).

## 7. Conclusion

The elaborate examples of the different utilizations of the FSSs in antenna engineering prove without any doubt the reliability and flexibility of these structures and their ability to enrich antenna research field, which can lead to further innovations. Meanwhile, the reliability and flexibility of FSSs make them very sensitive. Hence, their design should be performed carefully to attain the desired purposes.

In this chapter, we presented a proposed technique to gradually increase the gain of UWB planar antennas over frequency by using FSSs with low-profile subwavelength unit cells, thus eliminating the restriction of the UWB planar antennas to be used only for one to multiuser applications and extending their potential applications to include the ones where constant

and improved gain is required. The effectiveness of the proposed FSS-based reflectors has been proved using CPW-fed circular disc monopole as a radiator. A peak gain of 8.5 dBi with a maximum variation of 0.5 dBi across the UWB band has been achieved with a maintained wide bandwidth.

The proposed reflectors can also be of great importance for applications where the operation environment of the antennas can impact their behavior. The proposed reflectors can be used as shields to prevent the distortion of antenna behaviors. These reflectors, specially the UWB FSS reflector, can be used separately for UWB applications; therefore, a design guide of these types of structures has been proposed, which can be generalized to serve designing further UWB FSSs.

For further improvement of the UWB FSS-based antenna design, a new methodology of design was followed, which consists of designing the UWB FSS reflector and the UWB radiator together. As a result, an antenna with a small size (10*10 $cm^2$) and low profile of 10 mm, which corresponds to λ/10 at the lower frequency of operation, was obtained. This antenna can operate over the entire UWB band with unidirectional radiation characteristics and a peak gain varying from 8.5 to 10.5 dBi.

## Author details

Rabia Yahya*, Akira Nakamura and Makoto Itami

*Address all correspondence to: rabiamintsidi@yahoo.fr

Tokyo University of Science, Tokyo, Japan

## References

[1] Capolino F. Theory and Phenomena of Metamaterials. Boca Raton: CRC Press, Taylor and Francis Group; 2009

[2] Goussetis G, Feresidis AP, Vardaxoglou JC. Tailoring the AMC and EBG characteristics of periodic metallic arrays printed on ground dielectric substrate. IEEE Transactions on Antennas and Propagation. 2006;**54**(1):82-89

[3] Munk BA. Frequency Selective Surfaces: Theory and Design. New York: John Wiley & Sons Inc; 2000

[4] Pasian M, Monni S, Neto A, Ettorre M, Gerini G. Frequency selective surfaces for extended bandwidth backing reflector functions. IEEE Transactions on Antennas and Propagation. 2010;**58**(1):43-50

[5] Erdemli YE, Sertel K, Gilbert RA, Wright DE, Volakis JL. Frequency-selective surfaces to enhance performance of broad-band reconfigurable arrays. IEEE Transactions on Antennas and Propagation. 2002;**50**(12):1716-1724

[6] Ranga Y, Matekovits L, Esselle KP, Weily AR. Multioctave frequency selective surface reflector for ultra wideband antennas. IEEE Antennas and Wireless Propagation Letters. 2011;**10**:219-222

[7] Ranga Y, Esselle KP, Matekovits L, Hay SG. Increasing the gain of a semicircular slot UWB antenna using an FSS reflector. Antennas and Propagation in Wireless Communications. 2012

[8] Ranga Y, Matekovits L, Esselle KP, Weily AR. Design and analysis of frequency-selective surfaces for ultrawideband applications. EUROCON. 2011

[9] Ranga JY, Matekovits L, Weily AR, Esselle KP. A constant gain ultra-wide band antenna with a multi-layer frequency selective surface. Progress in Electromagnetics Research Letters. 2013;**38**:119-125

[10] Engheta N, Ziolkowski RW. Metamaterials Physics and Engineering Explorations. John Wiley & Sons, Inc; 2006

[11] Yahya R, Nakamura A, Itami M. Single-layer UWB FSS for enhancing the gain of UWB monopole antenna. In: 2015 IEEE International Conference on Ubiquitous Wireless Broadband (ICUWB). 2015. pp. 1-5

[12] Yahya R, Nakamura A, Itami M. Compact single-layer UWB frequency selective surface. In: AP-S/URSI 2016. 2016. pp. 957-958

[13] Liang J, Guo L, Chiau CC, Chen X, Parini CG. Study of CPW-fed circular disc monopole antenna for ultra wideband applications. IEE Proceedings-Microwaves, Antennas and Propagation. 2005;**152**(6):520-526

[14] Yang F, Rahmat-Samii Y. Electromagnetic Band Gap Structures in Antenna Engineering. UK: Cambridge University Press; 2008

[15] Foroozesh A, Shafai L. Investigation into the application of artificial magnetic conductors to bandwidth broadening, gain enhancement and beam shaping of low profile and conventional monopole antennas. IEEE Transactions on Antennas and Propagation. 2011; **59**(1):4-20

[16] Yahya R, Nakamura A, Itami M. Dual-polarized UWB antenna with unidirectional radiation. In: 2016 IEEE International Conference on Ubiquitous Wireless Broadband (ICUWB). 2016. pp. 1-3

[17] Yahya R, Nakamura A, Itami M, Denidni TA. A novel UWB FSS-based polarization diversity antenna. IEEE Antennas and Wireless Propagation Letters. 2017;**16**:2525-2528

[18] Yahya R, Nakamura A, Itami M, Denidni TA. Dual-polarized ultra-wideband antenna with improved polarization purity. ITE Transactions on Media Technology and Applications. 2016;**4**(4):363-368